Chapter 3

Device fabrication and measurement techniques

3.1 Introduction

The advance of the electron beam lithography technique permits nowadays fabrication of nano-scale devices. This makes possible to study spin dependent electron transport in metals, in which the relevant length scale for spin transport is of the order of 500 nm at room temperature. In this chapter, we give a detailed description of the various device fabrication methods and measurements techniques. The chapter is divided into three main sections. First, we discuss the experimental techniques necessary to fabricate our devices. Second, we describe the exact fabrication procedure of each device used in the remaining of this work. In the last section, the measurement techniques are discussed.

3.2 Device fabrication techniques

The fabrication process can be divided into two main steps: (i) The creation of an evaporation mask using electron beam lithography (EBL), (ii) metal deposition with subsequent lift-off.

3.2.1 Creating an evaporation mask using electron beam lithography

We used two different resist recipes in combination with EBL to fabricate the evaporation masks [1]. The main steps in the fabrication procedure are schematically shown in Fig. 3.1.

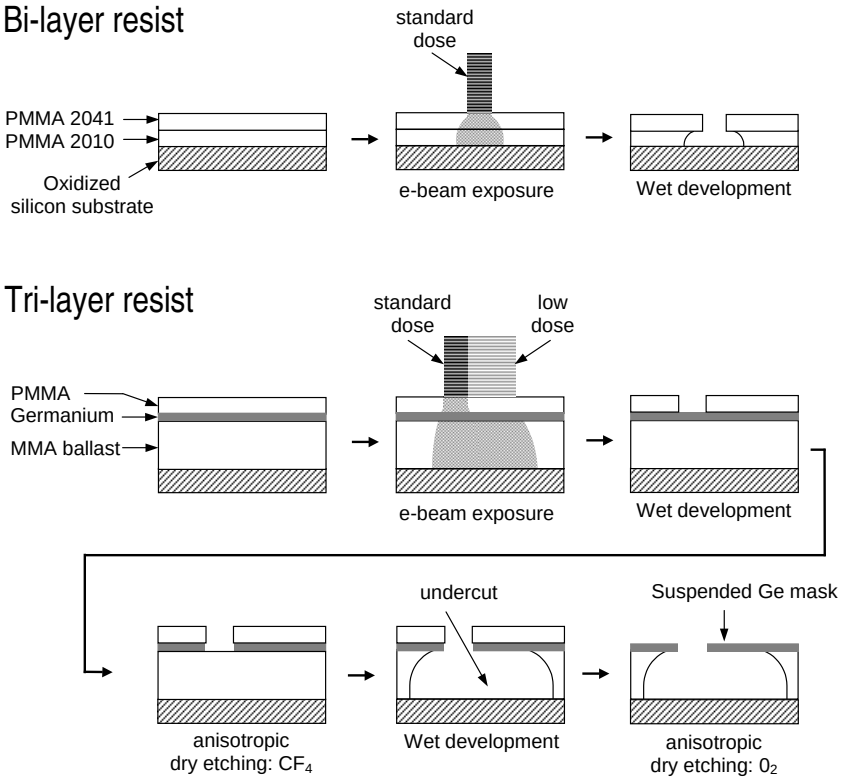

Figure 3.1: *Schematic of the fabrication steps of evaporation mask. The top row shows the bi-layer resist system. The following rows show the tri-layer resist system used to create a suspended Ge mask with defined undercuts for shadow depositions [1].*

Bi-layer resist

- First an organic resist layer is spun onto a Si substrate, polymethyl methacrylate (PMMA) 2010 (Du Pont Elvacitate, medium molecular weight), 4% in clorobenzene, or 8% in n-butyl acetate, and subsequently baked at 170°C for 10 minutes.

- A second organic resist, PMMA 2041 (Du Pont Elvacitate, high molecular weight) dissolved in 2.2% O-xylene is spun on top of the first one and baked for 30 minutes at same temperature. O-xylene is a weak solvent and hence it is used to prevent intermixing of the two layers. The typical thickness of the total bilayer is 300 to 400 nm.

- Then the device pattern is written using focussed e-beam. This breaks the polymer chains in the resist and the exposed parts can be subsequently removed by developing the sample for 60 seconds in a 1:3 solution of MIBK (methyl-isobutyl-ketone) and IPA (2-propanol). Electrons backscattered at the substrate interface and a lower molecular

mass cause the bottom resist to be developed faster than the top one. This forms a resist profile with a small undercut, which is important for a good lift-off.

Tri-layer resist

To achieve a larger and more stable undercut we have used a tri-layer resist. Here, a Ge layer will form the actual mask as it has the required mechanical strength to form a large suspended mask. This recipe is used for the fabrication of devices with shadow mask evaporation technique [1, 2]. Angle shadow evaporation is a necessary technique for fabrication of tunnel barriers between the contacts in a controlled way.

- In the first step (Fig. 3.1), a copolymer PMMA/MMA 33% dissolved in methoxy-ethanol is spun onto the wafer and baked for 20 minutes at 170°C, producing a 1.1 μm thick layer.
- Second, a 40 nm Ge layer is evaporated on top of the bottom resist.
- Third, a 300 nm thick, 950K PMMA 2% in chlorobenzene is spun on top of Ge and baked for 10 minutes at 140°C.
- The bottom and top resist layers have different sensitivities for e-beam radiation, which enables a selective exposure by varying the induced charge dose (400 μC/cm^2 both layers, 100 μC/cm^2 bottom layer) by the e-beam using a low current beam of 40 pA (37 keV). In this way large undercuts under the Ge layer are created, which permits deposition of metals at large angles.
- After the sample pattern is written by e-beam, the top layer is developed in IPA:MIBK 3:1 for 45 seconds.
- This serves as a mask for the reactive ion etching of the Ge layer in a CF_4 plasma. The etching process (pressure 25 μBar at 40 W power for 45 seconds) is monitored using a laser interferometer.
- Next, the bottom layer is developed in IPA:MIBK 3:1 for 50 seconds.
- In the last step the top layer and any remaining polymer in the narrow openings are removed by oxygen plasma etching (pressure 9 μbar with 40 W power for $\sim$3 minutes).

3.2.2 Metal deposition and lift-off

The deposition of the metals (e.g. Py, Co, Al, Cu, Ge, Pt) is done in a e-beam evaporator with a base pressure of 10^{-7} mbar with deposition rates

of 0.1-1 nm/second. The principle of angle (shadow) evaporation technique is shown in Fig. 3.2. A sample holder positioned upside down that can be tilted and rotated is used. An example of the angle shadow evaporation process is presented in the following. This device was fabricated by four-angle evaporation of three different metals. Figure 3.3(left) shows a scanning electron micrograph (SEM) of the Ge mask prepared as describe above (Tri-layer resist), while the Fig. 3.3(right) shows the picture of the device. In the Fig. 3.3(left) the black color corresponds to the regions where Ge is etched and the whitish contour around the etched dark regions is the undercut. As shown in Fig. 3.3(left), in the center of the device the carved undercut formed a suspended Ge bridge. This is sustained by undeveloped resist located away of the central region. First, 15 nm thick Au layer is deposited from below under an angle of 45° with the substrate surface. In this way two Au strip are formed, see the SEM picture. Second, an Al layer is deposited from the left side under an angle of 65° and another Al layer from right side under an angle of $-65°$. In this way a continuous Al strip (40 nm thick) underneath the suspended Ge bridge is formed. Third, without breaking the vacuum, an Al_2O_3 oxide layer is formed at the Al surface by exposing the sample to $2 \cdot 10^{-2}$ mbar pressure of pure O_2 for few minutes. Next, a Co (60 nm thick) layer is deposited from the top under an angle of $-45°$ in such way that overlaps with the Au strips deposited first.

The final step in the fabrication process is lift-off. In this step the remaining resist is dissolved by immersing the sample in hot (50°C) acetone for 15 minutes. Then, the sample is rinsed in cold acetone and dried with a nitrogen flow. Figure 3.3(right) shows a SEM image of a device after lift-off.

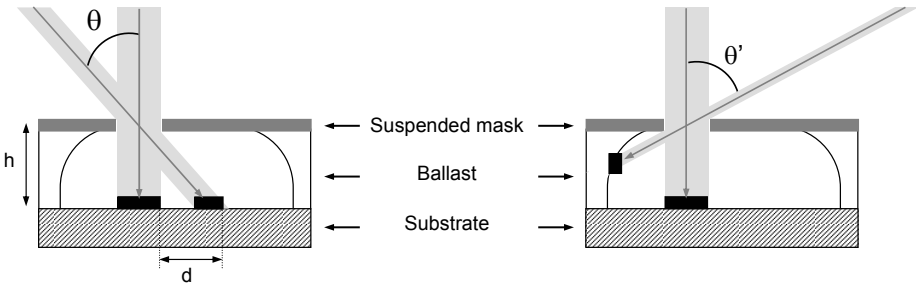

Figure 3.2: *The principle of shadow (angle) evaporation technique. Left, the evaporations are done one perpendicular and one under an angle θ, the resulting structures are shifted by a distance d. Right, at large angles the metal is deposited onto the side wall of the resist, and therefore removed upon lift-off [1].*

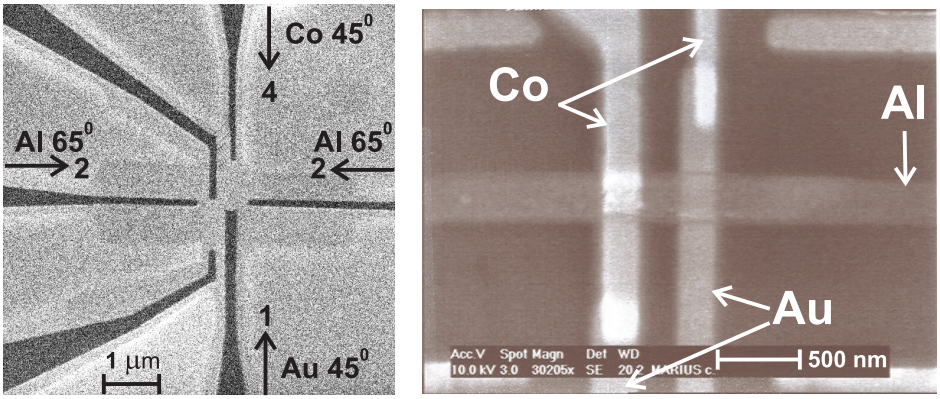

Figure 3.3: *Left, top view of the suspended Ge mask design to fabricate a lateral spin valve device shown in the right panel, via four angle shadow evaporation process. The dark regions which appear in the electron micrograph correspond to regions where the Ge is etched (openings in Ge). The metal deposition angles are as shown. Right, a SEM image of the finished device which consist of a strip of Al crossed by a Au and a Co strip.*

3.3 Fabrication procedure for the individual samples

In this section we describe in detail the fabrication process of two different types of devices studied in this thesis, **Device A** and **Device B**. For the **Device B** type, the angle evaporation technique was used in the fabrication process. Devices are fabricated on p-doped Si wafers with a 500 nm thick thermally grown SiO_2 insulating layer on the top.

3.3.1 Device A

The **Device A** fabrication necessitates four separate EBL steps for the different circuitry parts. The device consists of a single permalloy strip connected by four (see Chapter 6) or two (see Chapter 5 and Chapter 7) nonmagnetic leads for ac and dc measurements. Close to the ferromagnetic strip a thick metallic wire, i.e coplanar strip waveguide (CSW), is used for ac magnetic field generation. We proceed as follows:

step 1: **CSW and contacts.** A 2″ Si wafer is cleaved into small chips (∼2×2 cm). One chip is cleaned with hot acetone for 5 minutes, then placed on a hotplate at 150°C for 5 minutes. 950K PMMA (AllResist AR-P 671.04) 2% in chlorobenzene, is spun at 4000 rpm (300-400 nm thick) for 60 seconds and subsequently baked at 170°C for 30 minutes. Here,

only one resist layer is used because the metal is evaporated perpendicular and the undercut is not crucial. Then the design (pattern) is written into the resist by focused e-beam, for this step we use a probe current of 1 nA (with 10 keV) and a magnification of 50×. We developed in a 3:1 (IPA:MIBK) solution for 60 seconds. The developed chip is loaded into the e-beam evaporator, and 3 nm Ti and 150 nm Au are deposited. Ti creates a good adhesion of the Au layer. A 150 nm thick Au film is necessary for the CSW in order to allow a high density ac current to pass trough it. After lift-off in acetone about 6×2 patterns are created, each consists of 4 wirebond pads continued with leads, 4 markers and a CSW, see Fig. 3.4(left). Markers are necessary for alignment in subsequent EBL steps.

step 2: Permalloy strip. We use same resist system as is step 1, e-beam with a probe current of 19 pA and 500× magnification, e-gun evaporation and lift-off to deposit a single permalloy strip, 20-40 nm thick with 0.3×3 μm^2 lateral size, see Fig. 3.4(right).

step 3: Pt electrodes. Next, the conventional bi-layer resist (described in Fig. 3.1) is used. It is necessary to use as a bottom layer PMMA 2010 dissolved in n-butyl acetate in order to prevent the milling of the Py surface. Prior to deposition of the 30 - 60 nm thick Pt contacts layer (Fig. 3.4(right)), the Py surface is *insitu* cleaned by Argon ion milling, using an acceleration voltage of 500 V with a current of 10 mA for 30 seconds, removing the oxide and few nm of Py material to ensure transparent contacts. A gentle lift-off process is required.

step 4: Al electrodes. Same conventional PMMA bi-layer resist as in the previous step is used. An 170 nm thick Al layer is deposited to connect the Pt contact strips to Ti/Au leads. *Insitu* Ar etching is used prior to the Al leads deposition to clean the Pt and Au surface.

Figure 3.4 shows SEM images of the device for the intermediate fabrication steps.

3.3.2 Device B

EBL with angle evaporation technique was employed to fabricate **Device B** type. The spin valve device **Device B1** (see Chapter 4), consists of an aluminium island connected by means of four cobalt electrodes through the tunnel barriers. The **Device B2** (see Chapter 8) consists of a cobalt strip connected by four aluminium electrodes.

step 1: CSW and/or contacts. In the first step, 8 leads connected to large bonding pads and two coplanar waveguides (only for Device

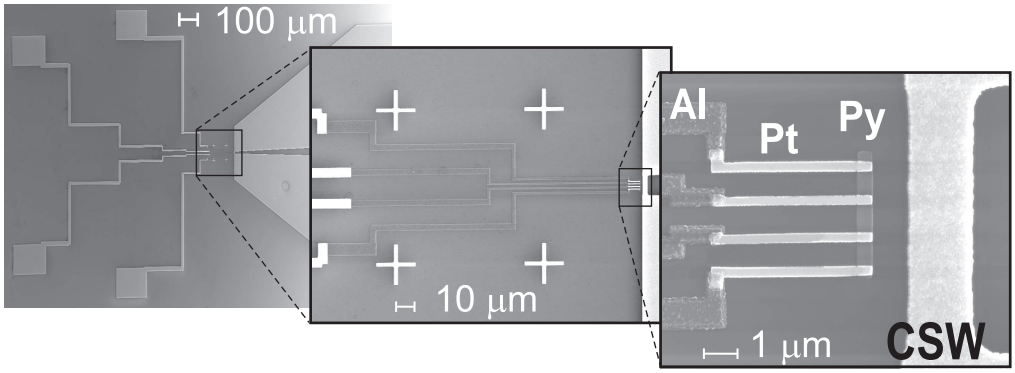

Figure 3.4: *SEM images of a lateral mesoscopic device, Device A. A series of progressive magnification are shown. Left, overall view of the 2×2 mm device, showing 4 wirebond pads and a coplanar strip waveguide (CSW), 150 nm gold thick. Middle, the gold leads coverage via aluminium leads (poor visible) into the center of the device. The 4 markers used for alignment are visible here. Right, close view of the central region which consists of a 35 nm thick permalloy ferromagnetic strip positioned close to the CSW and contacted by four platinum strips.*

B2) consisting of 5 nm Ti and 40 nm Au are fabricated using UV-optical lithography and e-gun evaporation. We used a optimized optical lithography recipe with a resolution down to ∼1 μm. However, due to the low reproductivity factor and acquisition of a new e-beam machine later we replaced UV-optical lithography step with e-beam lithography.

step 2: Tri-layer resist. We used the conventional tri-layer resist process to create a suspended Ge mask on top of 1.2 μm thick PMMA-MMA base layer with precise predefined undercuts.

step 3 ′: Al strip, oxidization and Co electrodes. For Device B1, we evaporated through the suspended mask 20 nm of Al at an angle of 35° to form a strip of 1 μm × 150 nm lateral size. Next, we expose Al to pure oxygen at a pressure of 10^{-2} mbar for 10 minutes to form a thin Al_2O_3 layer. In the last step, without breaking the vacuum, four Co electrodes 50 nm thick are deposited perpendicular to the substrate to connect the Al strip, see Fig. 3.5(a).

step 3 ″: Co strip and Al electrodes. For Device B2, the metal deposition is reversed. First a 40 nm thick Co strip with lateral size 2 μm × 130 nm is evaporated perpendicular to the substrate, deposited close and parallel to the coplanar waveguide. Next, in the same vacuum cycle, four Al fingers are deposited under an angle of 28° to form

clean contacts with the Co strip, see Fig. 3.5(b).

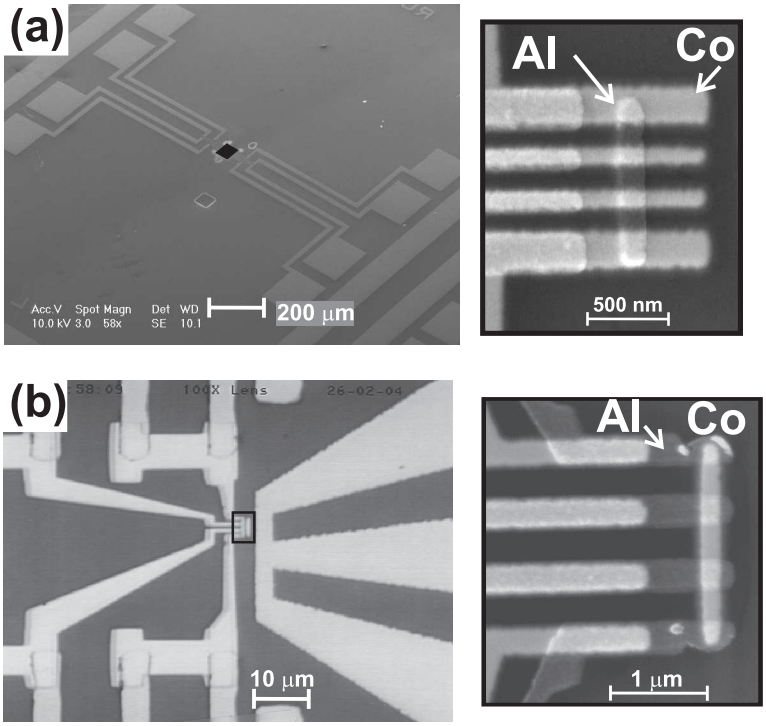

Figure 3.5: *SEM images of the lateral spin valve devices, (a) Device B1 and (b) Device B2. At the right, are close view of the central regions.*

After lift-off, the chip is cut in 2.5×2.5 mm small chips, each containing one complete device. The chips are glued to a standard 16 pin chip carrier. Electrical connections from the chip to the chip-carrier are made by ultrasonic bonding using Al/Si(1%) wires. The high frequency connections are made by a microwave probe.

3.4 Measurement techniques

Spin transport measurement in metals can be performed also at room temperature. Except for the measurements presented in Chapter 4, all measurements have been performed at room temperature.

The low frequency measurement electronics consists mainly of a lock-in amplifier (Stanford Research 830) and a home made voltage to current (V-I) convertor with a differential voltage amplifier. Four terminal current controlled measurements (for low resistive devices) are done using standard lock-in method: a reference ac voltage with a specific frequency from the lock-in is fed to the V-I convertor, next depending on the control feed back

resistance a current (10 nA to 1 mA rms) is sent to the device. The detected voltage is amplified by the differential voltage amplifier (with common mode rejection ratio of 120 dB) up to 10^4 and measured with the lock-in. Measurements are controlled by using a GPIB interface to a computer running LabView. At low temperatures the measurements have been performed in a dilution refrigerator with base temperature of 100 mK. Noise filtering on each wire is achieved by three RC low pass filters is series (each with 4 KΩ resistance and 1 nf capacitance) and a copper powder filter. Higher magnetic fields up to 8 T are achieved with a superconducting magnet.

On-chip generation of microwave magnetic fields.

To generate high frequency signals a microwave signal generator (R&S SMR40) is used which covers a frequency range from 10 MHz to 40 GHz and for power detection a spectrum analyzer (R&S FSP40) with operating frequencies from 9 KHz to 40 GHz with 1 Hz to 10 MHz resolution bandwidth. The transmission rf lines which guide rf signals from the signal generator to

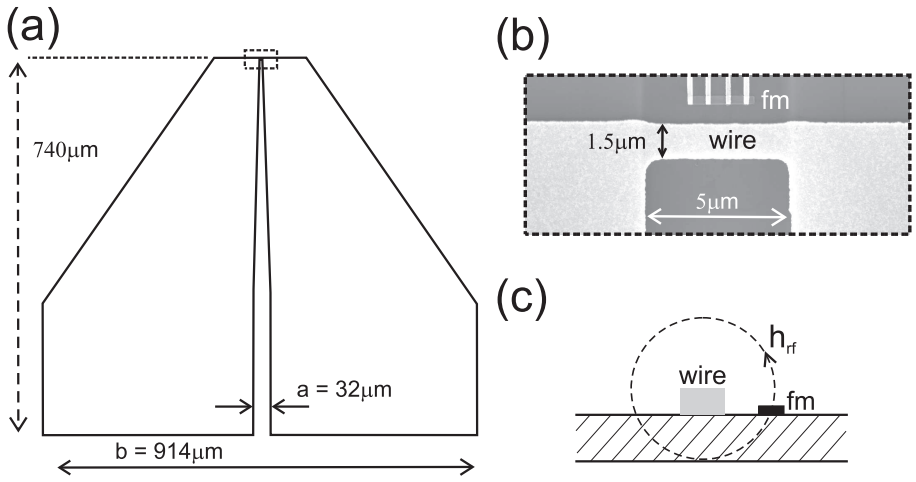

Figure 3.6: *(a) Schematic diagram of the on chip coplanar strip waveguide (CSW). The CSW is terminated by a narrow wire that shorts the two planes. The wire acts as a shorted termination of the* 50 Ω *transmission line and therefore the highest current density in the terminating short and thereby generating a microwave magnetic field. (b) SEM picture of a device, visible are the termination of the CSW as well as ferromagnetic strip connected with four contacts. (c) Schematic drawing of the cross-section of the CSW and ferromagnetic strip deposited on the top of the* Si/SiO_2 *substrate.*

termination with minimal losses consist of semirigid coaxial cables (Pasternack Enterprises, up to 26.5 GHz, non-magnetic), coplanar strip waveguide (CSW) fabricated on-chip, and the connection between them. Special care needs to be given to these connections in order to minimize reflections. This is done via a microwave probe (GGB Industries, Picoprobe 40A, loss $<$ 1

dB, dc to 40 GHz).

A shorted CSW is used for generating a microwave magnetic field. The shorted CSW consists of two sheets (signal and ground line) of metal shorted at the end by a wire on the Si/SiO_2 surface of our chip design to carry electromagnetic fields in a large bandwidth over a long distance. Our EBL fabricated gold CSWs have thicknesses from 150 up to 300 nm. The CSW is designed to match 50 Ω characteristic impedance of the coax line, up to the shorted end, to minimize power loss due to reflections. We have done this by introducing a tapering in the wave guide structure. This is possible by changing the dimensions a and b (see Fig. 3.6(a)) but keeping the ratio (a/b) constant. We estimate this geometrical factor, using Ref. [3], to be 0.035. Since the end wire has an resistance of 1-5 Ω less than the characteristic impedance, it represents a shorted termination and the current is maximum at the wire. As shown in Fig. 3.6(c), by sending an alternating current trough an CSW an oscillating magnetic field is generated. By placing a ferromagnetic strip within one wavelength (which is a few mm at 30 GHz) from the wire, the ferromagnetic strip is in the near-field region and the electric field and magnetic field distribution produced by the ac current should be the same as for a dc current [4]. At a distance r (smaller than the wavelength) from the center of the wire, a current I through a wire with circular cross-section thus produces a magnetic field $b_{rf} = \mu_0 I/2\pi r$, and no electric field (μ_0 is the magnetic susceptibility in vacuum). If the wire is located at 1 μm away from the strip, we need a current of about 10 mA (9 dBm, rf power) to produce a 1 mT microwave field. Energy dissipation by high frequency currents in transmission lines takes place through ohmic, dielectric and radiation losses [4]. In our case the cross-section of the shorted wire is so small that the on-chip ohmic losses dominate; which are of the order of 10 μW for I=1 mA [5].

References

[1] F. J. Jedema, Ph.D. thesis, University of Groningen (2002).

[2] G. J. Dolan, Appl. Phys. Lett. **31**, 337 (1977).

[3] K. C. Gupta, R. Garg, I. Bahl, and P. Bhartia, *Microstrip Lines and Slotlines* (Arttech House, Inc., Norwood, MA, 1996).

[4] J. Jackson, *Classical electrodynamics* (Wiley, New York, 1998).

[5] L. Vandersypen, R. Hanson, L. W. van Beveren, J. Elzerman, J. Greidanus, S. D. Franceschi, and L. Kouwenhoven, *Quantum Computing and Quantum Bits in Mesoscopic Systems, Ch. 22* (Kluwer Academic Plenum Publishers, 2002).